Models of DNA C1′ Radicals. Structural, Spectral, and Chemical Properties of the Thyminylmethyl Radical and the 2′-Deoxyuridin-1′-yl Radical

Chryssostomos Chatgilialoglu,*,† Carla Ferreri,‡,† Rita Bazzanini,† Maurizio Guerra,*,† Seung-Yong Choi,§ Calvin J. Emanuel,§ John H. Horner,§ and Martin Newcomb*,§

Contribution from the I.Co.C.E.A., Consiglio Nazionale delle Ricerche, Via P. Gobetti 101, I-40129 Bologna, Italy, Dipartimento di Chimica Organica e Biologica, Università di Napoli "Federico II", Via Mezzocannone 16, I-80134 Napoli, Italy, and Department of Chemistry, Wayne State University, Detroit, Michigan 48202

Received May 22, 2000. Revised Manuscript Received July 18, 2000

Abstract: The thyminylmethyl radical and the 2′-deoxyuridin-1′-yl radical were studied. The former radical was produced in laser flash photolysis (LFP) studies from two precursors derived from thyminylacetic acid, the *N*-hydroxypyridine-2-thione ester (PTOC ester), and the phenylselenyl ester. The thyminylmethyl radical has an absorbance in the range 315−340 nm. The rate constant for its reaction with octadecanethiol in THF at ambient temperature determined by LFP methods is $(3.1 \pm 0.6) \times 10^7$ M^{-1} s^{-1}. The 2′-deoxyuridin-1′-yl radical was produced in bulk photolyses from both diastereomers of the corresponding C1′ *tert*-butyl ketone, 1′-pivaloyl-2′-deoxyuridine, and in LFP studies from one diastereomer. Trapping of this C1′ radical with 2-mercaptoethanol, cysteine, or glutathione gave both anomers of 2′-deoxyuridine; the product ratios were similar in each case and insensitive to precursor identity or thiol concentrations. Rate constants for reactions of the 2′-deoxyuridin-1′-yl radical with thiols and metal ions were determined by LFP methods; the respective rate constants for reactions with 2-mercaptoethanol, cysteine, glutathione, $CuCl_2$, and $FeCl_3$ in water at ambient temperature are $(2.3 \pm 0.5) \times 10^6$, $(2.9 \pm 0.4) \times 10^6$, $(4.4 \pm 0.3) \times 10^6$, $(7.9 \pm 0.3) \times 10^7$, and ca. 1×10^8 M^{-1} s^{-1}. The 2′-deoxyuridin-1′-yl radical was addressed computationally. The radical center is not planar, and an energy profile for interconversion of the two anomeric forms of the radical was produced. Computed vertical transitions for the thyminylmethyl radical and one anomer of the 2′-deoxyuridin-1′-yl radical are in good agreement with the experimentally measured UV−visible spectra.

Abstraction of a hydrogen atom from the C1′ position of the sugar backbone of DNA is one of the events in the mechanism of action of various chemical nucleases and diffusible hydroxyl radicals generated by ionizing radiation.[1] Scheme 1 shows the reaction manifold for the C1′ radicals.[1,2] These reactions have been discussed over the last two decades, but only recently have quantitative measurements been possible from selectively generated species. Under anoxic or hypoxic conditions, a C1′ radical (**1**) may abstract a hydrogen atom from a thiol to give a mixture of α- and β-anomers (**2**).[3] The absolute rate constant for the reaction of 2′-deoxyuridin-1′-yl radical with glutathione (GSH) has recently been reported to be 4.4×10^6 M^{-1} s^{-1} at 20 °C.[4]

Scheme 1

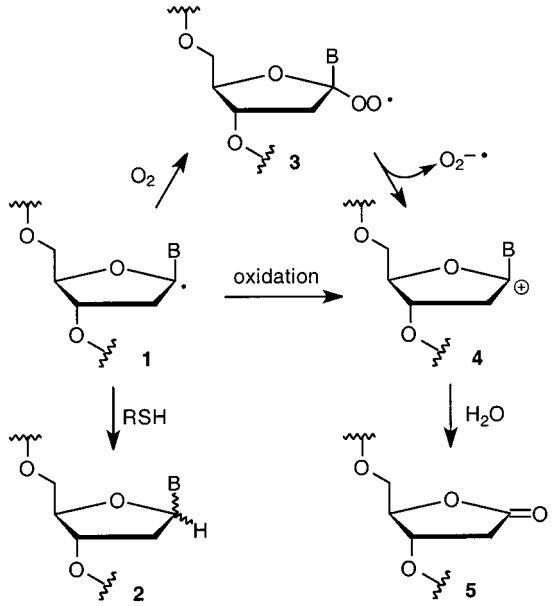

The formation of α-deoxynucleosides as misrepaired products has important consequences. For example, α-deoxyadenosine has been shown to be premutagenic in vitro since it directs novel nucleoside misincorporation during DNA replication.[5]

† Consiglio Nazionale delle Ricerche.
‡ Università di Napoli "Federico II".
§ Wayne State University.

(1) The subject is quite active at the present. (a) For an early discussion, see: von Sonntag, C. *The Chemical Basis of Radiation Biology*; Taylor & Francis Inc.: Philadelphia, PA, 1987 and references therein. (b) For some reviews in the past decade, see: Goldberg, I. H. *Acc. Chem. Res.* **1991**, *24*, 191−198. Nicolaou, K. C.; Dai, W.-M. *Angew. Chem., Int. Ed. Engl.* **1991**, *30*, 1387−1416. Knorre, D. G.; Fedorova, O. S.; Frolova, E. I. *Russ. Chem. Rev.* **1993**, *62*, 65−86. Pratviel, G.; Bernadou, J.; Meunier, B. *Angew. Chem., Int. Ed. Engl.* **1995**, *34*, 746−769. Breen, A. P.; Murphy, J. A. *Free Radical Biol. Med.* **1995**, *18*, 1033−1077. Pogozelski, W. K.; Tullius, T. D. *Chem. Rev.* **1998**, *98*, 1089−1107. Burrows, C. J.; Muller, J. G. *Chem. Rev.* **1998**, *98*, 1109−1151.

(2) C1′-radical-based approaches for the synthesis of modified nucleosides have also been reported. For example, see: Chatgilialoglu, C.; Gimisis, T.; Spada, G. P. *Chem. Eur. J.* **1999**, *5*, 2866−2876. Gimisis, T.; Ialongo, G.; Chatgilialoglu, C. *Tetrahedron* **1998**, *54*, 573−592.

10.1021/ja001783r CCC: $19.00
Published on Web 09/13/2000

In the presence of metal complexes or molecular oxygen, radical **1** leads to abasic site damage with the formation of a 2-deoxyribonolactone residue.[1,6] This lesion, which is alkaline-labile and results in strand scission,[1,6] has been reported to be mutagenic and resistant to repair nucleases.[7] The mechanistic aspects of the C1′ radical reactions under aerobic conditions have been studied in some detail including quantitative kinetic measurements. The reaction of the 2′-deoxyuridin-1′-yl radical with molecular oxygen gives the peroxyl radical **3** with a rate constant of 1×10^9 M^{-1} s^{-1}, which releases superoxide with a rate constant of ca. 2×10^4 s^{-1} to give the C1′ carbocation **4** (Scheme 1).[4,8] Quenching of the cation with water gives the lactone **5**, via an unstable hemiaminal.

Chemical nucleases of copper[9] and manganese[10] complexes are known to produce strand break under anoxic conditions. The involvement of radical **1** in the reaction of the 1,10-phenathroline−cuprous complex, $(o\text{P})_2\text{Cu}^+$, with hydrogen peroxide as a coreactant, and its further oxidation by Cu^{2+} to give the cation **4** is well assessed,[11] although kinetic information is lacking, and the fate of cation **4** is currently under dispute.[11,12] Evidence has been reported that the oxidation of the C−H bond in the C1′ position of DNA by manganese porphyrin behaves differently.[13] Initially, the H1′ abstraction by the Mn^{V}═O species generates radical **1** with Mn^{IV}−OH. The oxidation of radical **1** by Mn^{IV}−OH to give cation **4** seems to be unimportant with respect to the rebound mechanism (cytochrome P-450-like chemistry) to form the hemiaminal moiety directly. Chemistry at the C1′ position has also been considered for the iron complex of methidium-propyl-EDTA in the presence of molecular oxygen (or hydrogen peroxide) and reductant in a manner similar to $(o\text{P})_2\text{Cu}^+$ chemistry.[14−16]

Scheme 2

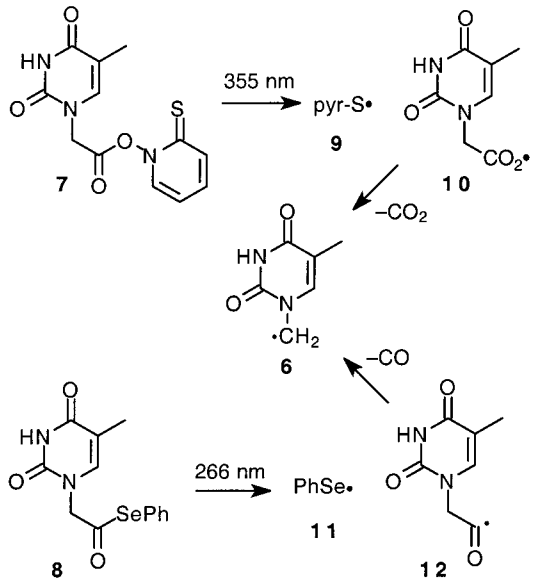

Our groups have studied the spectroscopy and chemistry of models of C1′ DNA radicals with the aim of determining the structural and reactivity effects of the base and the base coupled with the ethereal oxygen atom. We report here the preparations, UV−visible spectra, and chemical reactivities of a simple model, the thyminylmethyl radical, and a more complex model, the 2′-deoxyuridin-1′-yl radical, and we also address the latter from a computational perspective. In preliminary communications, we reported the EPR and UV−visible spectra of the latter and absolute rate constants for its reactions with thiols.[4,17]

Results and Discussion

Thyminylmethyl Radical. The thyminylmethyl radical (**6**) (see Scheme 2) is a simple DNA C1′ radical model with which one can evaluate the effects of the base on the radical center. Due to the relative ease of preparation of precursors to this radical, it was employed in LFP studies aimed at establishing protocols for spectral measurements and kinetic studies.

Two precursors to radical **6** were prepared from the known thyminylacetic acid, the PTOC ester[18] **7**, and the phenylselenyl ester[19] **8** (Scheme 2). The initial products from photolysis of **7** are the pyridine-2-thiyl radical (**9**) and acyloxyl radical **10** that will decarboxylate "instantly" on the nanosecond time scale to give **6**.[20] Photolysis of the phenylselenyl ester **8** initially produces the phenylselenyl radical (**11**) and the thyminylacetyl radical (**12**).[19] Decarbonylation of radical **12** to give radical **6** was expected to be slow enough to measure with nanosecond resolution.

Figure 1 shows time-resolved spectra obtained with precursors **7** and **8**. Figure 1A shows the decay of absorbances over a 6 μs

(3) Deeble, D. J.; Schulz, D.; von Sonntag, C. *Int. J. Radiat. Biol.* **1986**, *49*, 915−926. Lesiak, K. B.; Wheeler, K. T. *Radiat. Res.* **1990**, *121*, 328−337. Hwang, J.-T.; Greenberg, M. M. *J. Am. Chem. Soc.* **1999**, *121*, 4311−4315.

(4) Emanuel, C. J.; Newcomb, M.; Ferreri, C.; Chatgilialoglu, C. *J. Am. Chem. Soc.* **1999**, *121*, 2927−2928.

(5) Ide, H.; Yamaoka, T.; Kimura, Y. *Biochemistry* **1994**, *33*, 7127−7133. Ide, H.; Tedzuda, K.; Shimzu, H.; Kimura, Y.; Purmal, A. A.; Wallace, S. S.; Kow, Y. W. *Biochemistry* **1994**, *33*, 7842−7847.

(6) For some recent communications see: Tronche, C.; Goodman, B. K.; Greenberg, M. M. *Chem. Biol.* **1998**, *5*, 263−271. Doddridge, Z. A.; Warner, J. L.; Cullis, P. M.; Jones, G. D. D. *Chem. Commun.* **1998**, 1997−1998. Doddridge, Z. A.; Cullis, P. M.; Jones, G. D. D.; Malone, M. E. *J. Am. Chem. Soc.* **1998**, *120*, 10998−10999. Kotera, M.; Bourdat, A.-G.; Defrancq, E.; Lhomme, J. *J. Am. Chem. Soc.* **1998**, *120*, 11810−11811.

(7) For example, see: (a) Povirk, L. F.; Goldberg, I. H. *Proc. Natl. Acad. Sci. U.S.A.* **1985**, *82*, 3182−3186. (b) Povirk, L. F.; Houlgrave, C. W.; Han, Y.-H. *J. Biol. Chem.* **1988**, *263*, 19263−19266.

(8) (a) Chatgilialoglu, C.; Gimisis, T. *Chem. Commun.* **1998**, 1249−1250. (b) Tallman, K. A.; Tronche, C.; Yoo, D. J.; Greenberg, M. M. *J. Am. Chem. Soc.* **1998**, *120*, 4903−4909. (c) Greenberg, M. M. *Chem. Res. Toxicol.* **1998**, *11*, 1235−1248. (d) Chatgilialoglu, C. *Nucleosides Nucleotides* **1999**, *18*, 547−553.

(9) Sigman, D. S. *Acc. Chem. Res.* **1986**, *19*, 180−186. Sigman, D. S.; Mazumder, A.; Perrin, D. M. *Chem. Rev.* **1993**, *93*, 2295−2316.

(10) Meunier, B. *Chem. Rev.* **1992**, *92*, 1411−1456. Bernadou, J.; Pratviel, G.; Meunier, B. In *DNA and RNA Cleavers and Chemotherapy of Cancer and Viral Diseases*; Meunier, B., Ed.; Kluwer: Dordrecht, 1996; pp 211−223.

(11) Meijler, M. M.; Zelenko, O.; Sigman, D. S. *J. Am. Chem. Soc.* **1997**, *119*, 1135−1136. Zelenko, O.; Gallagher, J.; Sigman, D. S. *Angew. Chem., Int. Ed. Engl.* **1997**, *36*, 2776−2778.

(12) Chen, T.; Greenberg, M. M. *J. Am. Chem. Soc.* **1998**, *120*, 3815−3816. Oyoshi, T.; Sugiyama, H. *J. Am. Chem. Soc.* **2000**, *122*, 6313−6314.

(13) Pitié, M.; Bernadou, J.; Meunier, B. *J. Am. Chem. Soc.* **1995**, *117*, 2935−2936.

(14) Hertzberg, R. P.; Dervan, P. B. *Biochemistry* **1984**, *23*, 3934−3945. See also: Stubbe, J.; Kozarich, J. W. *Chem. Rev.* **1987**, *87*, 1107−1136 and references therein.

(15) Other metal complexes have also been reported to cleave DNA sugar oxidation at the 1′ position including, for example, oxoruthenium(IV)[16a] and oxochromium(V)[16b] derivatives.

(16) (a) Neyhart, G. A.; Cheng, C.-C.; Thorp, H. H. *J. Am. Chem. Soc.* **1995**, *117*, 1463−1471. (b) Bose, R. N.; Fonkeng, B. S. *Chem. Commun.* **1996**, 2211−2212.

(17) Chatgilialoglu, C.; Gimisis, T.; Guerra, M.; Ferreri, C.; Emanuel, C. J.; Horner, J. H.; Newcomb, M.; Lucarini, M.; Pedulli, G. F. *Tetrahedron Lett.* **1998**, *39*, 3947−3950.

(18) The acronym PTOC is for pyridine-2-thione-*N*-oxycarbonyl. See: Barton, D. H. R.; Crich, D.; Motherwell, W. B. *Tetrahedron* **1985**, *41*, 3901−3924.

(19) For a review of the chemistry of acyl radicals including phenylselenyl ester chemistry, see: Chatgilialoglu, C.; Crich, D.; Komatsu, M.; Ryu, I. *Chem. Rev.* **1999**, *99*, 1991−2069.

(20) PTOC esters have been used in a number of LFP applications; see: Horner, J. H.; Tanaka, N.; Newcomb, M. *J. Am. Chem. Soc.* **1998**, *120*, 10379−10390 and references therein.

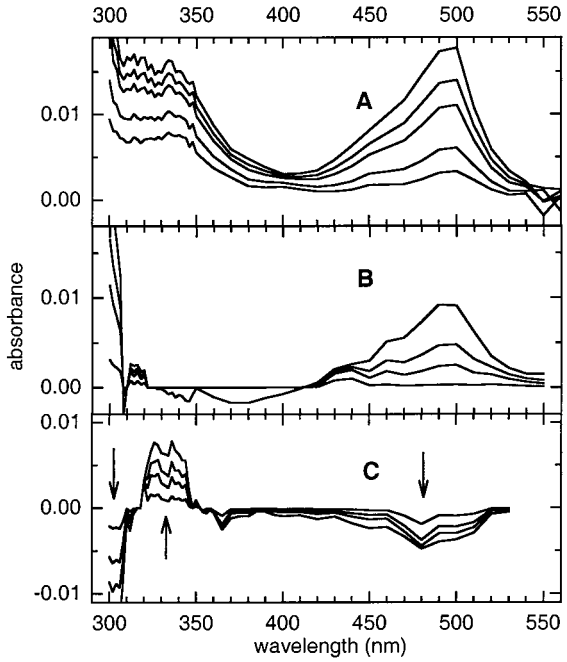

Figure 1. (A) Decay spectra between 0.43 and 6.0 μs after 355 nm photolysis of THF solutions of precursor **7** with the spectrum at 18 μs subtracted to give a baseline. (B) Decay spectra between 0.26 and 4.5 μs after 355 nm photolysis of the PTOC ester from octanoic acid in THF with the spectrum at 9 μs subtracted to give a baseline. (C) Time-resolved spectrum between 0.5 and 2.5 μs after 266 nm irradiation of precursor **8** in THF.

period following 355 nm photolysis of **7**. A late-time spectrum was subtracted from earlier spectra to remove the negative signals from bleaching of the precursor. Signals from the thiopyridyl radical at 300 and 490 nm[21] are decaying somewhat more rapidly than the signal in the 315−340 nm range. The 315−340 nm absorbance was absent in the spectrum obtained under similar conditions following photolysis of the PTOC ester of octanoic acid (Figure 1B), and we ascribe it to the thyminylmethyl radical (**6**).

Photolysis of the phenylselenyl ester **8** in THF with 266 nm laser light gave the time-resolved spectrum over 2.5 μs shown in Figure 1C. In this case, the initial spectrum was subtracted from later spectra with the result that decaying signals appear as negative absorbances and growing signals appear as positive absorbances. The phenylselenyl radical, absorbing at 300 and 480 nm,[22] is decaying. The growing signal in the 315−340 nm region resembles the signal in Figure 1A both in shape and intensity, thus reinforcing the assignment of this absorbance to radical **6**. The observed rate constant for signal growth in the 315−340 nm region in Figure 1C was ca. 4×10^5 s^{-1}. When **8** was photolyzed in acetonitrile under otherwise similar conditions, the observed rate constant for signal growth in the 315−340 nm region was about half as large as that in THF, consistent with observations that the rates of decarbonylations of acyl radicals decrease with increasing solvent polarity.[23a]

The observed rate constant for signal growth is the sum of all rate constants for loss of radical **12** (i.e. both decarbonylation to **6** and radical−radical couplings and disproportionations). We estimate that the rate constant in THF for decarbonylation of **12** is approximately 2×10^5 s^{-1}. For comparison, decarbonylation of the $HOCH_2C(=O)^\bullet$ radical has a rate constant in the range of 3×10^4 s^{-1} at ambient temperature,[23b] and the increased rate of decarbonylation of radical **6** relative to that of the $HOCH_2C(=O)^\bullet$ radical is noteworthy, especially in light of the similar kinetics for reactions of the product radicals with simple thiols (see below).

Scheme 3

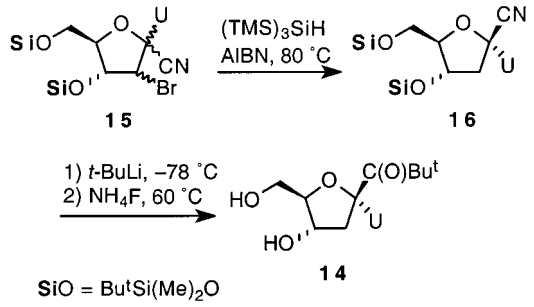

Further confirmation of the production of the thyminylmethyl radical was obtained in a product study. A radical chain reaction of PTOC ester **7** in THF in the presence of 0.8 M *t*-BuSH with visible light irradiation for initiation gave 1-methylthymine in 91% yield as determined by GC analysis.

The thyminylmethyl radical was also used in an exploratory study of thiol trapping kinetics. PTOC ester **7** was photolyzed in the presence of varying concentrations of octadecanethiol in THF, and the rate constant for reaction of **6** with the thiol, determined from a plot of k_{obs} versus thiol concentration, was $(3.1 \pm 0.6) \times 10^7$ M^{-1} s^{-1}. The rate constant for reaction of an α-methoxy radical with the same thiol in THF is 1×10^7 M^{-1} s^{-1}.[24] In the next section, we comment on the relative reactivities of models of C1′ radicals.

2′-Deoxyuridin-1′-yl Radical. As precursors for the selective generation of two conformations of this radical, we prepared the ketones **13** and **14**. We recently reported a three-step synthesis of **13** starting from one of the diastereomers of **15**.[8a,25] A mixture of diastereomers of **15** was prepared analogously following a literature procedure.[26] Then, **15** was debrominated by $(TMS)_3SiH$ under normal free radical conditions, and the resulting mixture of two diastereomers was separated by silica gel chromatography (Scheme 3). Short treatment of **16** with an excess of *t*-BuLi yielded, after silica gel purification, the protected *tert*-butyl ketone as the major product.[25] Finally, deprotection (NH_4F, methanol, 60 °C) produced the water soluble adduct **14**.

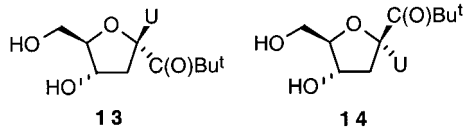

Products from the reactions of the 2′-deoxyuridin-1′-yl radical with thiols were determined in continuous photolysis reactions.

(21) Alam, M. M.; Watanabe, A.; Ito, O. *J. Org. Chem.* **1995**, *60*, 3440−3444.

(22) Chatgilialoglu, C. In *Electronic Absorption Spectra of Free Radicals*; Scaiano, J. C., Ed.; CRC Press: Boca Raton, FL, 1989; Vol. 2, pp 3−11.

(23) (a) Tsentalovich, Y. P.; Fischer, H. *J. Chem. Soc., Perkin Trans. 2* **1994**, 729−733. (b) Vollenweider, J.-K.; Paul, H. *Int. J. Chem. Kinet.* **1986**, *18*, 791−800.

(24) Tronche, C.; Martinez, F. N.; Horner, J. H.; Newcomb, M.; Senn, M.; Giese, B. *Tetrahedron Lett.* **1996**, *37*, 5845−5848.

(25) Chatgilialoglu, C.; Ferreri, C.; Gimisis, T. *Tetrahedron Lett.* **1999**, *40*, 2837−2840. Chatgilialoglu, C.; Costantino, C.; Ferreri, C.; Gimisis, T.; Romagnoli, A.; Romeo, R. *Nucleosides Nucleotides* **1999**, *18*, 637−639.

(26) (a) Haraguchi, K.; Itoh, Y.; Tanaka, H.; Yamaguchi, K.; Miyasaka, T. *Tetrahedron Lett.* **1993**, *34*, 6913−6916. (b) Itoh, Y.; Haraguchi, K.; Tanaka, H.; Gen, E.; Miyasaka, T. *J. Org. Chem.* **1995**, *60*, 656−662. (c) Yoshimura, Y.; Kano, F.; Miyazaki, S.; Asshida, N.; Sakata, S.; Haraguchi, K.; Itoh, Y.; Tanaka, H.; Miyasaka, T. *Nucleosides Nucleotides* **1996**, *13*, 305−324.

Table 1. Ratios of 2′-Deoxyuridine Anomers from Photolysis of Ketones **13** and **14** in the Presence of Thiols[a]

precursor	thiol	[RSH] (M)	β:α ratio	uracil (%)
13	CySH	0.04	65:35	2.8
		0.1	64:36	1.9
		0.4	65:35	2.0
13	$HO(CH_2)_2SH$	0.04	60:40	1.4
		0.1	61:39	1.3
		0.4	61:39	1.4
13	GSH	0.04	57:43	1.1
		0.1	57:43	1.2
		0.4	58:42	1.2
14	CySH	0.04	65:35	2.0
		0.1	66:34	1.6
		0.4	66:34	1.7

[a] Reactions in water at ca. 40 °C with 40−60% consumption of precursor. [b] The yields of 2′-deoxyuridine were >80% based on consumed precursor.

Scheme 4

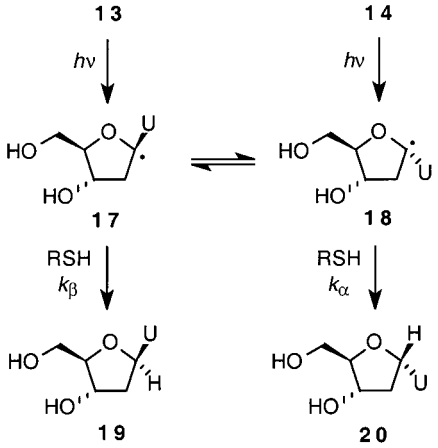

A Pyrex tube containing either ketone **13** or **14** (0.01 M) and the appropriate thiol in H_2O (200 mL) was deoxygenated and photolyzed in a Rayonet photochemical reactor at ca. 40 °C. After 90 min of photolysis, the sample was analyzed by HPLC or lyophilized and followed by ^{1}H NMR spectroscopic analysis. β-Mercaptoethanol, cysteine, and glutathione were used as the hydrogen donors. Table 1 shows the details of these experiments. The yields of 2′-deoxyuridine in all cases were greater than 80% based on the consumed starting material. The β:α anomeric ratio was found to be independent of the concentration of thiol in the range of 0.04−0.4 M. In the series of experiments using ketone **13**, the β:α ratio decreased slightly when CySH was replaced with GSH or $HOCH_2CH_2SH$. An identical β:α ratio was obtained by replacing the ketone **13** with **14** in the presence of CySH.

The factors controlling the stereochemical outcome of the reaction deserve some comment. Scheme 4 shows the reaction mechanism for these transformations. The initial radicals **17** and **18**, generated respectively from the corresponding ketones **13** and **14**, are expected to be in equilibrium since EPR spectroscopy and theoretical calculations show C1′ radicals to be pyramidal (vide infra). The subsequent reactions with a thiol afford the α- and β-anomers of 2′-deoxyuridine (i.e. **19** and **20**). The fact that the product ratio is independent of both the initial concentration of thiols and the starting ketone suggests that the C1′ radical is rapidly inverting, and the product distribution is controlled only by the difference between the total free energy of activation for each pathway (Curtin−Hammett principle).[27] The β/α distribution, therefore, should depend on the size of the shielding effect of the two γ-substituents in the sugar ring, i.e., OH vs CH_2OH.[28]

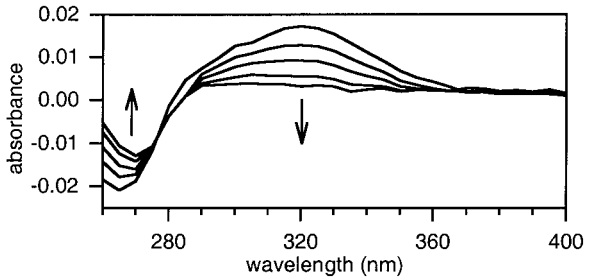

Figure 2. Time-resolved decay spectra following 266 nm irradiation of precursor **13** in a nonsparged water solution. The spectra are at 0.1, 0.9, 1.9, 3.9, and 8.9 μs after the laser pulse.

In addition to the H-atom trapped products, a small amount of the free base uracil (UH) was produced in the continuous irradiation experiments. A likely origin of the base is hydrolysis of 1′,2′-didehydro-2′-deoxyuridine (**21**).[29] Product **21** should be formed in disproportionation reactions of the C1′ radical with other radicals in the medium.

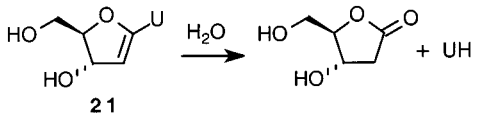

Laser flash photolysis experiments provided the UV−visible spectrum and reaction kinetics of the 2′-deoxyuridin-1′-yl radical. Irradiation of ketone **13** with 266 nm light (Nd:YAG) in aqueous solutions resulted in "instant" formation of a transient with an absorbance centered at 320 nm that we ascribe mainly to the rapidly equilibrating mixture of radicals **17** and **18** (Figure 2). The bleaching centered at 264 nm in the spectra is due to destruction of precursor **13**. The *tert*-butyl radical is reported to have a weak absorbance at 315 nm and a stronger absorbance at 260 nm,[23a,30] and irradiation of di-*tert*-butyl ketone under conditions similar to those employed with **13** resulted in only a small signal at 320 nm. The triplet excited state of uracil in water displays a weak signal with λ_{max} at 360 nm,[31] but we observed no absorbance in this region when an aqueous solution of uracil was irradiated under the conditions used for photolysis of **13**. The decay of the 320 nm absorbance in the presence of oxygen without a concomitant growth in the "bleached" region of the spectrum further indicates that the observed absorbance was not due to an excited state. Finally, the good agreement between computed (vide infra) and observed spectra for **17**, as well as for **6**, supports the assignment.

In principle, cleavage of ketone **13** can occur at either side of the carbonyl group to give either the C1′ radical and the pivaloyl radical or the *tert*-butyl radical and the C1′-acyl radical. If the latter pathway occurred at all, then decarbonylation to the C1′ radical must have been very fast because no noticeable signal growth occurred at 320 nm following the initial burst. Rate constants for decarbonylations of acyl radicals are known to be strongly affected by the overall enthalpies of the reactions

(27) Seeman, J. I. *Chem. Rev.* **1983**, *83*, 83−134.
(28) Curran, D. P.; Porter, N. A.; Giese, B. *Stereochemistry of Radical Reactions*; VCH: Weinheim, 1995.
(29) Robins, M. J.; Trip, E. M. *Tetrahedron Lett.* **1974**, 3369−3372. Haraguchi, K.; Tanaka, H.; Maeda, H. Itoh, Y.; Saito, S.; Miyasaka, T. *J. Org. Chem.* **1991**, *56*, 5401−5408.
(30) Chen, T.; Paul, H. *J. Phys. Chem.* **1985**, *89*, 2765−2767.
(31) Salet, C.; Bensasson, R. *Photochem. Photobiol.* **1975**, *22*, 231−235.

Table 2. Rate Constants for Reactions of the 2′-Deoxyuridin-1′-yl Radical and the Hydroxymethyl Radical[a]

	rate constant (M^{-1} s^{-1})	
trapping agent	2′-deoxyuridin-1′-yl	$HOCH_2^{\bullet}$ [b]
oxygen	2×10^9 [c]	4.9×10^9
$HOCH_2CH_2SH$	$(2.3 \pm 0.5) \times 10^6$	1.3×10^8 [d]
cysteine	$(2.9 \pm 0.4) \times 10^6$	1.0×10^8
glutathione	$(4.4 \pm 0.3) \times 10^6$	$(0.4-1.0) \times 10^8$
Cu^{2+}	$(7.9 \pm 0.3) \times 10^7$	1.6×10^8
Fe^{3+}	ca. 1×10^8	8.0×10^7

[a] Reactions in neutral water at (22 ± 2) °C. [b] Data from refs 34 and 35. [c] Reference 17. [d] At pH 10.

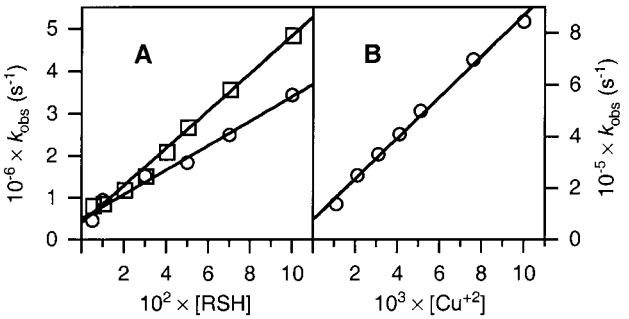

Figure 3. Observed rate constants for decay of the 2′-deoxyuridin-1′-yl radical in the presence of trapping agents at (22 ± 2) °C. (A) Reactions in the presence of cysteine (circles) and glutathione (squares). (B) Reactions in the presence of $CuCl_2$.

with little, if any, entropy differences found for widely divergent examples,[19] and decarbonylation of the putative C1′-acyl radical would be expected to be faster than decarbonylation of radical **12**, the immediate precursor to the thyminylmethyl radical.

Kinetic studies of the 2′-deoxyuridin-1′-yl radical were possible, and the results are collected in Table 2. When **13** was photolyzed in He-sparged aqueous solutions, the signal decay at 320 nm was slow as expected for radical−radical reactions with the low concentrations of transients produced in the LFP experiment. Typically, a biexponential decay with apparent first-order rate constants of 1×10^4 and 5×10^4 s^{-1} was observed. In nonsparged solutions with an estimated O_2 concentration of 0.3 mM, signal decay was greatly accelerated.[17] From the observed rate of decay, we calculated a rate constant for reaction of the C1′ radical with oxygen at 23 °C of 1×10^9 M^{-1} s^{-1}.[17] This rate constant is similar to those found for reaction of oxygen with a variety of α-heteroatom-substituted radicals in water.[32]

Rate constants for reactions of the thiols 2-mercaptoethanol, cysteine, and glutathione were measured. When precursor **13** was photolyzed in He-sparged aqueous solutions containing various concentrations of the thiols, the rate of signal decay from the C1′ radical increased smoothly with increasing concentrations of the thiols. Figure 3A shows the results from reactions conducted in the presence of cysteine and glutathione. The slopes of these lines gave the second-order rate constants for thiol reactions with the C1′ radical that are collected in Table 2. The ratio of rate constants for reaction of the radical with 2-mercaptoethanol and oxygen computed from our results ($k_H/k_T = 2.3 \times 10^{-3}$) is in good agreement with the ratio found in competition experiments by Greenberg.[33]

LFP studies of reactions of the C1′ radical with metal ions were precluded for most metals by their absorbances at 266 nm. Copper(II) was an exception. Figure 3B shows the observed rate constants for decay of the 320 nm signal when the C1′ radical was produced at 22 °C in water in the presence of varying concentrations of $CuCl_2$. The data give a second-order rate constant for the oxidation reaction of $(7.9 \pm 0.3) \times 10^7$ M^{-1} s^{-1}. LFP studies also were possible at low concentrations of $FeCl_3$; a crude rate constant for reaction of the C1′ radical with Fe^{3+} of 1×10^8 M^{-1} s^{-1} was obtained.

Kinetic studies of DNA C1′ radical models in water have been reported previously. Most of these results were obtained from pulse radiolysis studies where the radicals of interest were generated by hydrogen atom abstraction by the highly reactive hydroxyl radical. Therefore, C1′ DNA radical models have typically been simple species such as the hydroxymethyl radical produced from methanol. Table 2 contains rate constants for reactions of the hydroxymethyl radical with the various agents studied here.[34,35] The rate constants for reactions of the 2′-deoxyuridin-1′-yl and hydroxymethyl radicals with oxygen are similar; oxygen trapping is quite fast, and the values for these two radicals are typical for α-heteroatom radicals.[32]

The rate constants for oxidation of the 2′-deoxyuridin-1′-yl radical by Cu^{2+} and Fe^{3+} also are similar to those for oxidation of the hydroxymethyl radical.[34,35] In the oxidation reactions, the C1′ cation produced from the 2′-deoxyuridin-1′-yl radical will be considerably more stable than the cation from the hydroxymethyl radical, and the oxidation would be expected to be much faster for the C1′ system if the kinetics were influenced primarily by enthalpy changes. Such a kinetic effect was seen, for example, in the rate constant for release of superoxide from the 2′-deoxyuridin-1′-peroxyl radical.[4] The rate constants for oxidations of the series of α-hydroxyalkyl radicals from methanol, ethanol, and 2-propanol by Cu^{2+} decrease in a manner suggestive of an inner-sphere electron-transfer process involving bond-forming steps,[34b] and such an explanation would be in accord with the measured rate constant for oxidation of the 2′-deoxyuridin-1′-yl radical. The rate constants for Fe^{3+} oxidation of the α-hydroxyalkyl radicals from methanol, ethanol, and 2-propanol increase somewhat for the series,[34a,c] but our results with the 2′-deoxyuridin-1′-yl radical again suggest an inner-sphere process sensitive to steric effects. Because the steric constraints about the C1′ position of 2′-deoxynucleoside-1′-yl radicals should be similar, the rate constants we obtained for metal ion oxidations of the 2′-deoxyuridin-1′-yl radical should be good estimates for other C1′ deoxynucleoside radicals.

In the case of thiol reactions with the 2′-deoxyuridin-1′-yl radical, the kinetics appear to be sensitive to the enthalpy of the reaction, and the rate constants for the C1′ radical are about 2 orders of magnitude smaller than those for reactions of the hydroxymethyl radical. It is noteworthy that the major components affording stabilization to the C1′ radical, the alkoxy group and the base, do not have similar kinetic effects on thiol trappings when separated from one another. We noted that the rate constants for octadecanethiol trapping of the thyminylmethyl radical and an α-methoxy radical in THF were comparable,[24] and the rate constant for reaction of an alkyl radical with the same thiol in THF has about the same value.[24] In addition, the

(32) Marchaj, A.; Kelley, D. G.; Bakac, A.; Espenson, J. H. *J. Phys. Chem.* **1991**, *95*, 4440−4441. Das, S.; Schuchmann, M. N.; Schuchmann, H.-P.; von Sonntag, C. *Chem. Ber.* **1987**, *120*, 319−323. Hiller, K.-O.; Asmus, K.-D. *J. Phys. Chem.* **1983**, *87*, 3682−3688. Willson, R. L. *Trans. Faraday Soc.* **1971**, *67*, 3008−3019. Adams, G. E.; Willson, R. L. *Trans. Faraday Soc.* **1969**, *65*, 2981−2987.

(33) Goodman, B. K.; Greenberg, M. M. *J. Org. Chem.* **1996**, *61*, 2−3.

(34) (a) Buxton, G. V.; Green, J. C. *J. Chem. Soc., Faraday Trans. 1* **1978**, *74*, 697−714. (b) Cohen, H.; Meyerstein, D. *J. Am. Chem. Soc.* **1972**, *94*, 6944−6948. (c) Grodkowski, J.; Neta, P.; Schlesener, C. J.; Kochi, J. K. *J. Phys. Chem.* **1985**, *89*, 4373−4378.

(35) Ross, A. B.; Mallard, W. G.; Helman, W. P.; Buxton, G. V.; Huie, R. E.; Neta, P. NDRL-NIST Solution Kinetic Database, Ver. 3, Notre Dame Radiation Laboratory, Notre Dame, IN, and NIST Standard Reference Data, Gaithersburg, MD 1998.

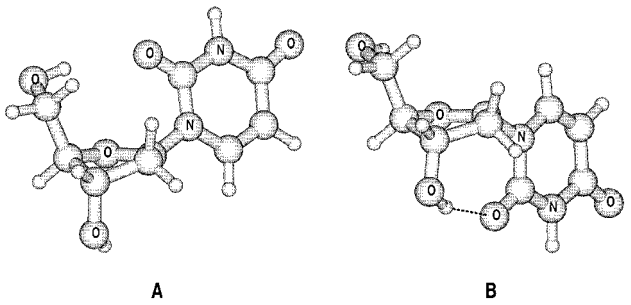

Figure 4. UHF/6-31G* geometries of the preferred conformations of the 2′-deoxyuridine-1′-yl radical: (A) $_3$E form of the β-anomer and (B) $_3$T^4 form of the α-anomer.

rate constants for reactions of the hydroxymethyl radical with various thiols in water are similar to that for reaction of the glutathione diethyl ester with an alkyl radical in an 80:20 water/acetonitrile mixture (6×10^7 M^{-1} s^{-1}).[24] Thus, the base and an alkoxy or hydroxy group have essentially no net kinetic effects on thiol trapping as individual substituents despite the fact that they stabilize a radical center. In previous studies of thiol reactions with radicals, the absence of a kinetic effect for an α-alkoxy group on the radical and the observation of polar solvent effects on the kinetics were interpreted in terms of a polarized transition state for H-atom transfer from thiols and increased nucleophilicity of an α-alkoxy radical over an alkyl radical.[24]

MO Calculations. Molecular orbital (MO) calculations have been carried out on the 2′-deoxyuridin-1′-yl radical to obtain information on its structural properties and to assign the hyperfine coupling (hfs) constants determined by ESR spectroscopy and the optical transitions observed in the UV−vis region of the LFP spectrum. The preferred conformations of the β- and α-anomer of the 2′-deoxyuridin-1′-yl radical determined with ab initio calculations at the UHF/6-31G* level of theory are shown in Figure 4.

The puckering mode of the sugar ring in DNA is usually described in terms of the endocyclic torsion angles ν_i ($i = 0-4$), the phase angle of pseudorotation P, and the maximum torsion angle ν_m.[36] For the β-anomer (Figure 4A), the computed values are ν_0 −1.9°, $\nu_1 = 22.2°$, $\nu_2 = -32.7°$, $\nu_3 = 32.3°$, $\nu_4 = -19.7°$, $P = 195.5°$, and $\nu_m = 33.9°$. These values indicate that the 2′-deoxyuridin-1′-yl radical adopts the C3′-exo puckering mode ($_3$E envelope form). This result is in contrast to those obtained studying C1′ radicals in which the base is modeled by an amino group.[37] The ab initio calculations performed on C1′ radical models predict a C2′-endo puckering mode (^{2}E envelope form). The presence of the pyrimidinic base slightly increases the pseudorotation phase angle from ca. 162° (^{2}E form) to ca. 198° ($_3$E form), that is, at the upper bound of the domain of the puckering modes experimentally observed in nucleosides and nucleotides ($137° < P < 194°$).[33] The uracil base adopts the syn orientation, with the molecular plane being roughly orthogonal to the ring moiety. The dihedral angle χ(O4′C1′N1C2), which denotes the orientation of the base relative to the sugar, is computed to be 61.0°. This is in contrast with what was experimentally found in nucleosides and nucleotides where a pyrimidinic base adopts an anti conformation, and both syn and anti conformations were found for purinic bases.[38,39]

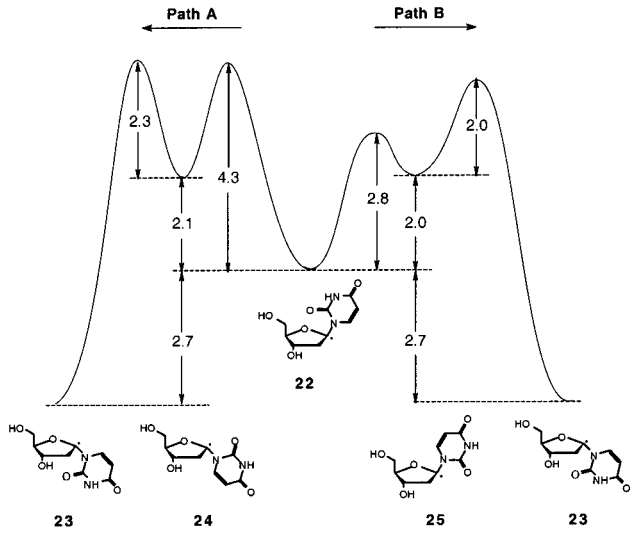

Figure 5. Energy profiles (kcal/mol) for the interconversion between the preferred conformations of the β- and α-anomers of the 2′-deoxyuridin-1′-yl radical calculated at UHF/6-31G*.

The computed values of the puckering parameters for the α-anomer ($\nu_0 = 6.2°$, ν_1 12.3°, $\nu_2 = -24.1°$, $\nu_3 = 28.4°$, $\nu_4 = -22.2°$, $P = 210.9°$, and $\nu_m = 28.1°$) indicate that the hydrogen bond (see Figure 4B) slightly increases the pseudorotation phase angle so that the preferred conformation tends to adopt the twist form $_3$T^4 with major C3′-exo and minor C4′-endo puckering. In the α-anomer, the base also adopts a syn orientation, and this conformation was computed to be more stable than the β-anomer by 2.7 kcal/mol (cf. structures **22** and **23** in Figure 5). A strong hydrogen bond between the O2 of the pyrimidinic base and the C3′ oxidrilic hydrogen (see Figure 4B) could be responsible for the greater stability of the α-anomer. Indeed, the distance of 2.01 Å between O2 and the C3′ oxidrilic hydrogen is much smaller than the 2.34 Å computed for the hydrogen bond in the β-anomer between O2 and the C5′ oxidrilic hydrogen. The molecular plane of the uracil base was computed to be perpendicular to the ring moiety ($\chi = 286.1°$).

The conversion between structures **22** and **23** is not a simple process (Figure 5). Inversion of configuration followed by a C−N bond rotation (path A) or a C−N bond rotation followed by inversion of configuration (path B) is necessary. The β-anomer, which adopts the anti conformation (**25**), was computed to be less stable than the syn conformation (**22**) by 2.0 kcal/mol, with the orientation of the uracil base being shifted by about 150° ($\chi = 205.3°$). The energy barrier between the two conformers (clockwise rotation) was computed to be 2.8 kcal/mol. The inversion barrier from **25** to **23** is 2.0 kcal/mol. On the other hand, the inversion barrier at the radical center C1′ for β-anomer **24** was computed to be relatively small (4.3 kcal/mol), whereas the rotation barrier between conformers **24** and **23** (clockwise rotation) was computed to be 2.3 kcal/mol. It is worth underlining that the energy difference between the α- and β-anomers for the less stable anti conformers, where the O2 atom is not involved in hydrogen bonds, is negligible. In this case the β-anomer was computed to be more stable than the α-anomer by 0.1 kcal/mol.

Hyperfine coupling (hfs) constants were computed for comparison to the experimental EPR spectrum.[17] We used the optimized UHF/6-31G* structure with the density functional (DFT) method at the UB3LYP/6-311G** level which was found

(36) Altona, C.; Sundaralingam, M. *J. Am. Chem. Soc.* **1972**, *94*, 8205−8212.

(37) (a) Miaskiewicz, K.; Osman, R. *J. Am. Chem. Soc.* **1994**, *116*, 232−238. (b) Colson, A.-O.; Sevilla, M. D. *J. Phys. Chem.* **1995**, *99*, 3867−3874.

(38) De Leeuw, H. P. M.; Haasnoot, C. A. G.; Altona, C. *Isr. J. Chem.* **1980**, *20*, 108−126.

(39) Sundaralingam, M. *Ann. N.Y. Acad. Sci.* **1976**, *255*, 3−42. Saenger, W. *Angew. Chem., Int. Ed. Engl.* **1973**, *12*, 591−601.

to provide reliable hfs constants with a modest computational effort.[40] The calculations indicate that the observed hfs constants (19.24 and 24.44 G)[17] should be assigned to the C2′ β-hydrogens (15.0 and 29.0 G at the UB3LYP/6-311G**//UHF/6-31G* level). The difference between the computed values of the two hfs constants is larger than that observed experimentally; however, the average values of the experimental (21.84 G) and computed (22.0 G) hfs constants are in excellent accord. Previous ab initio calculations of C1′ radical models gave slightly larger average hfs constants (22.6 G[37a] and 23.8 G[37b] for the ^{2}E puckering mode). The differences between the experimental and theoretical hfs values are probably due to the fact that vibrational effects have not been considered in the calculations. Actually, the pseudorotational motion of the five-membered ring is expected to decrease the difference between the two C2′ β-hydrogen hfs constants. For example, the prototype symmetric tetrahydrofuranyl radical[41,42] has β-hydrogen hfs constants in polycrystalline solution at 113 K[42] of 18.5 and 37.0 G, but the hfs constants are equivalent (28.2 G) at a temperature greater than 148 K[41] due to the averaging over the vibrational states. In the 2′-deoxyuridin-1′-yl radical, the presence of substituents at the 1′-, 3′-, and 4′-positions prevents the complete average of the two C2′ β-hydrogen hfs constants. However, the computed values are in agreement with the experimental values (16.1 and 28.0 G) observed for the 2′-deoxyguanosine 5′-monophosphate at 10 K[43] where vibrational effects due to pseudorotation and inversion at the radical center should be negligible. Interestingly, the calculated spin density in the p atomic orbitals of the radical center, $\rho_p(C1') = 0.685$, is only slightly higher than that estimated experimentally by the dipolar coupling tensor, $\rho_p(C1') = 0.636$.[43] Agreement between experiment and theory becomes very close if the C1′−H_β distance determined for the radical species at the UHF/6-31G* level (2.147 Å) is employed in estimating spin density from the dipolar coupling tensor, $\rho_p(C1') = 0.679$. Note that the total spin density at C1′ is computed to be much higher, $\rho(C1') = 0.798$, owing to the sizable contribution from the 2s atomic orbital deriving from the pyramidalization of the radical center.

The calculations indicate that the α-nitrogen hfs constant is small (1.5 G) because a negative spin density contribution due to spin polarization is counterbalanced by the positive contribution arising from the pyramidalization at the radical center. Hfs constants of γ-hydrogens are also predicted to be small (−0.4 G at H3′ and 0.2 G at H4′) because the hydrogens adopt equatorial positions. This finding is in agreement with the small values of the γ-hydrogen hfs constant (two equivalent hydrogens) observed in the prototype tetrahydrofuranyl radical (0.8 G for H3′ and 1.95 G for H4′).[42] These small couplings might contribute to the large experimental line widths observed in the EPR spectrum.[17]

The optical spectrum (transition wavelength λ and oscillator strengths f) of the C1′ radical **17** was computed with the time-dependent DFT method (TD-UB3LYP/6-311G**//UHF/6-31G*) which was shown to reproduce well the UV−vis spectra of large molecules.[44] The optical spectra of radicals **26** and **6** and 1-methyluracil (**27**) were also computed for comparison.

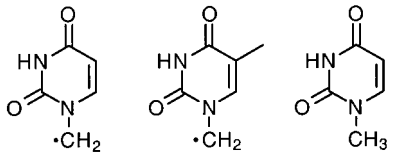

26 **6** **27**

Table 3 shows that the theoretical results are in good accord with the experimental findings. Indeed, comparison of the theoretical results for **26** and **6** indicates that the introduction of a methyl group at C5 in the uracil base should have little effect on the optical spectrum. More importantly, transitions in the region 300−400 nm are predicted by calculations of the optical spectrum of the C1′ radical **17** as well as for that of radical **6**, whereas in **27**, the longer wavelength transition is computed to occur near 240 nm.

In particular, the higher intensity transition in C1′ radical was computed at about 300 nm, that is, at a slightly shorter wavelength than observed experimentally. Calculations indicate that this transition is due to an excitation of the β-electron from the highest doubly occupied MO localized at the π system of the base (out-of-phase mixing between the N1 π lone pair and the π C═C orbital) to the singly occupied MO localized at C1′. The transition of the α-electron from the SOMO to the LUMO localized at the π^* system of the base (in-phase mixing of the π^* orbitals of the C═C and C═O bonds) occurs at a longer wavelength (about 400 nm) and with lower intensity. This transition was not observed in the LFP spectra of **17** and **20**, probably because it should occur at $\lambda > 400$ nm with low intensity. Indeed, the absorption spectra of the radical anion formed by deprotonation of radical **26**, obtained by pulse radiolysis of 1-methyluracil at pH 13.7, shows a weak band at a longer wavelength (λ_{max} about 450 nm) in addition to the strong absorption observed at about 300 nm.[45] TD-DFT calculations performed on this radical anion show that a weak transition should occur at $\lambda > 400$ nm ($\lambda = 433$ nm; $f = 0.005$), whereas a strong transition is predicted at about 300 nm ($\lambda = 309$ nm; $f = 0.189$) in agreement with experimental findings. The higher intensity transition in **27** is computed at a slightly shorter wavelength than that observed experimentally[46] as found above for the strongest transition in the C1′ radical. This is a transition to a singlet excited state due to excitation from the HOMO (π orbital of the base) to the LUMO (π^* orbital of the base). The forbidden transition to the corresponding triplet excited state is computed to occur at about 350 nm. Interestingly, this forbidden transition was observed as a weak signal at about 360 nm by 266 nm irradiation of a concentrated solution of uracil in water.[31]

Conclusions

DNA radicals have held the interest of chemists and biochemists for years,[1] and a large body of results exists for simple models of DNA C1′ radicals. The syntheses of photochemically sensitive precursors to specific base-substituted radicals such as the thyminylmethyl and 2′-deoxyuridin-1′-yl radicals permits a considerable advance in the sophistication of the models. The reasonably strong chromophores observed in the UV−vis spectra of both are in good agreement with computed values, and other C1′ nucleoside radicals should have

(40) Adamo, C.; Barone, V.; Fortunelli, A. *J. Chem. Phys.* **1995**, *101*, 384−393. Gauld, J. W.; Eriksson, L. A.; Radom, L. *J. Phys. Chem.* **1997**, *102*, 11352-1359.

(41) Trofimov, V. I.; Chkheidze, I. I. *Khim. Vys. Energ.* **1967**, *1*, 324−335; *High Energy Chem. USSR (Engl. Transl.)* **1967**, *1*, 282−291.

(42) Gaze, C.; Gilbert, B. C. *J. Chem. Soc., Perkin Trans. 2* **1978**, 503−508.

(43) Hole, E. O.; Nelson, W. H.; Sagstuen, E.; Close, D. M. *Radiat. Res.* **1992**, *129*, 119−138.

(44) Stratmann, R. E.; Scuseria, G. E.; Frisch, M. J. *J. Chem. Phys.* **1998**, *109*, 8218−8224.

(45) Ioele, M.; Chatgilialoglu, C.; Mulazzani, Q. G. *J. Phys. Chem. A* **1998**, *102*, 6259−6265.

(46) Aeby, D.; Suppan, P. *J. Chem. Soc., Faraday Trans.* **1994**, *90*, 3129−3138.

Table 3. Vertical Optical Transitions Computed at the UB3LYP/6-311G**//HF/6-31G* Level with the TD-DFT Method[a]

species	λ (nm)	f	transition[b]	expt (nm)
17	378	0.006	a	
	296	0.010	b	320
26	400	0.013	a	
	308	0.094	b	
6	405	0.011	a	
	318	0.106	b	330
27	236	0.167	c	261[c]

[a] Wavelengths (λ) and oscillator strengths (f) for transitions with $f > 0.005$. [b] Transition {spin}: a = SOMO $\rightarrow \pi^*$(base){α}; b = π(base) $\rightarrow$ SOMO{β}; c = π(base) $\rightarrow \pi^*$(base). [c] Reference 31.

similar absorbances. The kinetics obtained with the 2′-deoxyuridin-1′-yl radical are likely to provide good estimates for rate constants of reactions of other C1′ nucleoside radicals, especially with thiols that effect "repair" reactions. The good agreement between the structural features of the 2′-deoxyuridin-1′-yl radical found computationally and those indicated by the ESR spectrum of this radical[17] is noteworthy, particularly the pyramidalization at the radical center. This agreement suggests that structural features of other C1′ nucleoside radicals computed at the level of theory applied here will be reliable.

Experimental Section

(5-Methyl-2,4-dioxo-3,4-dihydro-2*H*-pyrimidin-1-yl)ethanoic Acid 2-Thioxo-2*H*-pyridin-1-yl Ester (7). A solution of (5-methyl-2,4-dioxo-3,4-dihydro-2*H*-pyrimidin-1-yl)ethanoic acid[47] (0.18 g, 0.98 mmol) and 2,2′-dithiobis(pyridine-*N*-oxide) (0.26 g, 1.07 mmol) in THF (10 mL) was cooled to 0 °C. The flask was shielded from light. Tributylphosphine (0.27 mL, 1.1 mmol) was added dropwise via syringe. The mixture was stirred at 0 °C for 1 h. Addition of benzene (1 mL) resulted in precipitation of **7**. The precipitate was filtered off and washed with hexane and benzene to give **7** as a yellow solid in 0.175 g (61%) yield. The sample was judged to be >95% pure by ^{1}H NMR. Mp 152−153 °C dec with gas evolution. ^{1}H NMR (acetone-d_6−DMSO-d_6): δ 1.84 (d, J = 1.2 Hz, 3 H), 5.00 (s, 2 H), 6.88 (td, J = 7.0, 1.8 Hz, 1 H), 7.43 (ddd, J = 8.5, 7.0, 1.5 Hz, 1 H), 7.56 (q, J = 1.2 Hz, 1H), 7.59 (dd, J = 8.5, 1.8 Hz, 1 H), 8.17 (dd, J = 7.3, 1.2 Hz, 1 H). ^{13}C NMR ($CDCl_3$−DMSO-d_6): δ 10.3 (CH_3), 45.0 (CH_2), 108.0 (C), 111.5 (CH), 133.1 (CH), 134.2 (CH), 137.1 (CH), 138.8 (CH), 149.1 (C), 162.5 (C), 163.0 (C), 172.6 (C).

***se*-Phenyl (5-Methyl-2,4-dioxo-3,4-dihydro-2*H*-pyrimidin-1-yl)-selenoethanoate (8).** Tributylphosphine (0.7 mL, 0.0028 mol) was added dropwise to a solution of methyl (5-methyl-2,4-dioxo-3,4-dihydro-2*H*-pyrimidin-1-yl)ethanoate[47a] (0.400 g, 0.0022 mol) and *N*-(phenylseleno)phthalimide (0.85 g, 0.00282 mol) in anhydrous DMF (15 mL) at 10 °C. The solution was stirred overnight at room temperature. DMF was removed under vacuum. Chloroform (4 mL) was added to the residue, and the resulting mixture was filtered to remove precipitated phthalimide. The chloroform was removed under vacuum, and the resulting crude product was chromatographed on silica gel (hexanes−acetone, 7:3) to give **8** contaminated with tributylphosphine oxide. Recrystallization from ethyl acetate−hexanes gave pure **8** as a white solid (0.28 g, 40%). Mp 181−182.5 °C. ^{1}H NMR (DMSO-d_6): δ 1.76 (s, 3 H), 4.75 (s, 2 H), 7.38−7.48 (m, 5 H), 7.58 (s, 1 H), 11.52 (bs, 1 H). ^{13}C NMR (DMSO-d_6): δ 12.0 (CH_3), 59.0 (CH_2), 109.3 (C), 124.5 (C), 129.4 (CH), 129.7 (CH), 135.8 (CH), 141.2 (CH), 150.9 (C), 164.3 (C), 197.4 (C). MS (ESI): 324.87 $(M + H)^+$, 346.84 $(M + Na)^+$, 670.87 $(2M + Na)^+$. MS (EI): *m*/*z* (rel intensity), 167 (49), 157 (23), 139 (48), 96 (100), 78 (68), 77 (51), 51 (33). HRMS (CI): calcd for $C_{13}H_{13}N_2O_3Se$ $(M + H)^+$, 325.0091; found, 325.0088.

Radical Reduction of a Mixture of Diastereoisomers of 15. To a magnetically stirred solution of **15** (500 mg; 0.92 mmol), as a 1:1.5 mixture of α- and β-anomers, in benzene (10 mL) kept under argon, were consecutively added tris(trimethylsilyl)silane (342 mg; 1.38 mmol) and AIBN (0.09 mmol; 15 mg). The reaction mixture was heated at reflux for 2 h. TLC (eluent: *n*-hexane/ethyl acetate 7/3) showed the consumption of the starting material. The solvent was evaporated under vacuum affording a syrup (α:β diastereoisomeric mixture of the reduced product) which was separated by silica gel flash-chromatography (*n*-hexane/ethyl acetate 8/2). A first fraction containing the α-anomer **16** (150 mg; 0.32 mmol; 35% yield) was eluted and evaporated under vacuum. Addition of hexane resulted in precipitation of white crystals. Mp 162−164 °C. ^{1}H NMR ($CDCl_3$): δ 0.01, 0.04, 0.13, 0.14 (s, each 3H, $SiMe_3$), 0.79, 0.94 (s, each 9H, $SiBu^t$), 2.94 (m, 2H, 2′-H), 3.74 (t, 2H, J = 2.8 Hz, 5′-H), 4.36 (m, 1H, 4′-H), 4.44 (m, 1H, 3′-H), 5.72 (d, 1H, J = 8.5 Hz, 5-H), 7.57 (d, 1H, J = 8.5 Hz, 6-H), 8.27 (bs, 1H, NH). ^{13}C NMR ($CDCl_3$): δ −5.7, −5.4, −5.1, −5.0 (each CH_3), 17.6, 18.3 (each C), 25.4, 25.9 (each 3 × CH_3), 47.4, 62.7 (each CH_2), 72.4 (CH), 88.2 (C), 93.4 (CH), 101.8 (CH), 115.4 (C), 137.9 (CH), 149.4, 163.0 (C). MS: *m*/*z* (rel intensity), 482 (5) $(M + 1)^+$, 424 (18), 261 (19), 187 (39), 169 (25), 89 (51), 73 (100). HR-MS: calcd for $(M - t\text{-Bu})^+$, 424.1724; found, 424.1719. A second fraction was eluted containing the β-anomer (220 mg; 0,47 mmol; 51% yield) which had spectral characteristics identical to those reported.[26c]

Preparation of Compound 14. To a magnetically stirred solution of **16** (150 mg; 0.31 mmol) in dry THF (0.5 mL), kept under argon at −78 °C, was slowly added *tert*-butyllithium (0.93 mmol; 0.6 mL of a 1.6 M solution in hexane) via syringe. The reaction was stirred for 30 min, then quenched by adding a saturated solution of 0.1 N HCl at low temperature and worked up by partitioning with ethyl acetate and water. The organic phase was dried with anhydrous sodium sulfate, and solvent was evaporated to afford an oil which was separated by silica gel flash chromatography (ethyl acetate/hexane 7/3). The first fraction gave the silylated compound **14** (16 mg; 20% yield based on the consumption of starting material). The silylated **14** was immediately dissolved in dry MeOH (5 mL), in a Wheaton reactor equipped with a stopper, with an excess of NH_4F (16 mg) and stirred at 60 °C overnight. The solvent was evaporated under vacuum, and the residue was chromatographed on silica gel with ethyl acetate increasing the amount of methanol up to 5%. The ketone **14** (7 mg; 77% yield) was further purified by preparative TLC with ethyl acetate/MeOH (95/5) as eluent. ^{1}H NMR (acetone-d_6): δ 1.15 (s, 9H, Bu^t), 2.12 (dd, 1H, J = 2.4, 14.4, 2′-H), 3.42 (dd, 1H, J = 5.6, 14.4 Hz, 2′-−H), 3.49 (m, 2H, 5′-H), 4.44 (m, 2H, 3′-H, 4′-H), 5.66 (d, 1H, J = 8.4 Hz, 5-H), 7.88 (d, 1H, J = 8.4 Hz, 6-H), 10.1 (bs, 1H, NH). ^{13}C NMR (CD_3CN): δ 29.5 (3 × CH_3), 42.2 (CH_2), 43.8 (C), 62.1 (CH_2), 71.8 (CH), 92.4 (CH), 100.7 (C), 101.4 (CH), 141.3 (CH), 151.4, 163.9, 204.1 (C). Anal. Calcd for $C_{14}H_{20}N_2O_6$ (C, H, N): 53.84, 6.45, 8.97. Found: 53.98, 6.44, 8.94.

Product Studies from Continuous Photolysis. A Pyrex tube containing the ketone **13** or **14** (0.01 M) and the appropriate thiol dissolved in H_2O (200 mL) was deoxygenated and photolyzed in a Rayonet photochemical reactor (equipped with six lamps of 350 nm) for 90 min at ca. 40 °C. The consumption of the ketone **13** or **14** and the formation of uracil and its derivatives **19** and **20** were followed by using HPLC analysis on a reverse-phase analytical column (Waters Spherisorb S5ODS2, 150 × 4.6 mm, 3 mm) using authentic samples as references. Absolute concentrations were interpolated from external standard calibration curves. In some experiments, the reaction mixture was lyophilized followed by ^{1}H NMR analysis. In all cases the agreement between the two techniques was found to be excellent. The consumption of the starting ketone varied between 40 and 60%, whereas the yields of 2′-deoxyuridine were higher than 80% based on the disappearance of the starting material. In all experiments, a small amount of free base was obtained. Table 1 shows the details of these experiments.

Laser Flash Photolysis. Laser flash photolysis experiments were performed on an Applied Photophysics LK-50 kinetic spectrometer employing a Nd:YAG laser with a 7 ns pulse with power of ca. 40 mJ/pulse at 266 nm and ca. 75 mJ/pulse at 355 nm. Dilute, He-sparged solutions of **10** or **12** in THF or of **13** in water (absorbances of ca. 0.4 AU at the irradiating wavelength) at (22 ± 2) °C were allowed to flow through the spectrometer cell. The solutions contained various concentrations of thiols or salts. Spectra were obtained in 2 or 5 nm steps.

(47) (a) Dueholm, K. L.; Egholm, M.; Behrens, C.; Christensen, L.; Hansen, H. F.; Vulpius, T.; Petersen, K. H.; Berg, R. H.; Nielsen, P. E.; Buchardt, O. *J. Org. Chem.* **1994**, *59*, 5767−5773. (b) Kosynkina, L.; Wang, W.; Liang, T. C. *Tetrahedron Lett.* **1994**, *35*, 5173−5176.

For kinetic studies, the maximum absorbance line found in the spectra was monitored. Typically, multiple spectra were summed to improve signal-to-noise. Typical standard errors in observed rate constants were <5%.

Computational Details. MO calculations were carried out with the GAUSSIAN 98 system of programs[48] running on a DEC-Alpha 500 computer. Geometries were optimized at the Hartree−Fock (HF) level using the 6-31G* valence-double-ζ basis set supplemented with polarization *d*-functions on heavy atoms.[49] Spin unrestricted wave functions were employed in calculations on radical species; however, spin contamination of the doublet state by higher spin multiplets is quite small, the expectation value of $\hat{S}^2$ being less than 0.76 for any radical.

Hfs constants and optical transitions were computed at the optimized geometry with the DFT method using the B3LYP hybrid functional[50] and the 6-311G** valence-triple-ζ basis set supplemented with polarization, *p*-functions on hydrogen, and *d*-functions on heavy atoms.[51]

Acknowledgment. This work was supported by the "Commitato CNR per le Scienze e Tecnologie dell' Informazione" (M.G.) and a grant from the National Institutes of Health (GM56511). C.C. and M.N. are grateful to NATO for a travel grant (CRG970142).

JA001783R

(48) Frisch, M. J.; Trucks, G. W.; Schlegel, H. B.; Scuseria G. E.; Robb, M. A.; Cheeseman, J. R.; Zakrzewski, V. G.; Montgomery, J. A., Jr.; Stratmann, R. E.; Burant, J. C.; Dapprich, S.; Millam, J. M.; Daniels, A. D.; Kudin, K. N.; Strain, M. C.; Farkas, O.; Tomasi, J.; Barone, V.; Cossi, M.; Cammi, R.; Mennucci, B.; Pomelli, C.; Adamo, C.; Clifford, S.; Ochterski, J.; Petersson, G. A.; Ayala, P. Y.; Cui, Q.; Morokuma, K.; Malick, D. K.; Rabuck, A. D.; Raghavachari, K.; Foresman, J. B.; Cioslowski, J.; Ortiz, J. V.; Stefanov, B. B.; Liu, G.; Liashenko, A.; Piskorz, P.; Komaromi, I.; Gomperts, R.; Martin, R. L.; Fox, D. J.; Keith, T.; Al-Laham, M. A.; Peng, C. Y.; Nanayakkara, A.; Gonzalez, C.; Challacombe, M.; Gill, P. M. W.; Johnson, B.; Chen, W.; Wong, M. W.; Andres, J. L.; Gonzalez, C.; Head-Gordon, M.; Replogle, E. S.; Pople, J. A. GAUSSIAN 98, Revision A.7, Gaussian, Inc., Pittsburgh, PA, 1998.

(49) Hariharan, P. C.; Pople, J. A. *Theor. Chim. Acta* **1973**, *28*, 213−222.

(50) Becke, A. D. *J. Chem. Phys.* **1993**, *98*, 5648−5652.

(51) Krishnan, R.; Binkley, J. S.; Seeger, R.; Pople, J. A. *J. Chem. Phys.* **1980**, *72*, 650−654.